ROCK PHYSICS AND MECHANICAL STRATIGRAPHY OF THE WOODFORD SHALE, ANADARKO BASIN, OKLAHOMA

By

BRIAN HENRY VARACCHI

Bachelor of Science in Geology

Oklahoma State University

Stillwater, Oklahoma

2005

Submitted to the Faculty of the
Graduate College of the
Oklahoma State University
in partial fulfillment of
the requirements for
the Degree of
MASTER OF SCIENCE
December, 2011

ROCK PHYSICS AND MECHANICAL

STRATIGRAPHY OF THE WOODFORD SHALE,

ANADARKO BASIN, OKLAHOMA

Thesis Approved:

Dr. Priyank Jaiswal

Thesis Adviser

Dr. Jim Puckette

Dr. Estella Atekwana

Dr. Sheryl A. Tucker

Dean of the Graduate College

.

ACKNOWLEDGMENTS

I would first like to thank the Boone Pickens School of Geology and Chesapeake Energy for providing the financial support for my graduate studies. I want to thank the Oklahoma City Geological Foundation for awarding me the Frederick H. and Lois M. Kate Endowment to provide partial support for my research. I give a sincere thanks to Laurie Geiger of TGS for providing me the data to complete this project, without her assistance and gratitude, this project would not have been possible. Additionally, I would like to thank my adviser Dr. Priyank Jaiswal, and committee members Dr. Jim Pucktte and Dr. Estella Atekwana for their knowledge and guidance. I would also like to acknowledge Jack Dvorkin from Standford University for his assistance and input on this project, Samiya Al Bulushi for her time and assistance in helping to develop some of the rock physics models, and my colleagues in the seismic lab. Last but not least I want to acknowledge the love and support of my family. Without them I would not be where I am today and I am extremely grateful for their ongoing guidance that pushed me to finish graduate school.

TABLE OF CONTENTS

LIST OF TABLES

Table Page

LIST OF FIGURES

CHAPTER 1

ABSTRACT

Application of seismic techniques in exploration of mudrocks is limited due to the lack of well-developed rock physics methods that can link the matrix and fluid properties to seismic velocities. We present a first principle based modeling method for predicting P- and S- wave velocities (V_P and V_S respectively) in mudrocks accounting for the effect of silica content, porosity, and free gas saturation. We apply the modeling method to real $V_P - V_S$ data from the Woodford Shale of the Anadarko Basin in the Mcneff 2-28 well, section 28, T.10N., R.6W., Grady County, Oklahoma to estimate the rock and fluid properties. Modeling suggests that the Woodford within the Mcneff 2-28 has high silica content (>60%), intermediate porosity (10 – 20%), and high gas saturation (90–85%). Although our estimate of gas saturation has uncertainty, estimated porosity and silica content are reasonable when compared to a suite of logs from the Mcneff 2-28 and a core from the Campbell 1-34, section 34, T.10N., R.6W., Grady County, Oklahoma (~1 mile SE of the Mcneff 2-28). We conclude that the Upper Woodford unit in the Mcneff 2-28 locality is potentially prospective.

CHAPTER 2

INTRODUCTION

Mudrocks are defined as fine- to very fine grained sedimentary rocks [*Grainger*, 1984]. Although the primary component of a mudrock matrix is clay, their overall composition can vary from dominantly siliceous to dominantly calcareous [*Blatt et al.*, 2005]. A large variation in matrix mineralogy and small clay/silt grain size makes experimental and numerical studies of mudrocks extremely challenging. However, their recently discovered hydrocarbon resource potential [*Charpentier and Cook*, 2010; *DOE*, 2009] combined with their widespread presence (>65% of all sedimentary rocks) have provided ample reasons for researchers to revisit the current understanding of their physical properties. Geochemical conditions related to Total Organic Carbon (TOC)[1] and thermal maturity that make mudrocks good hydrocarbon sources are generally well understood [*Hester and Schmoker*, 1987; *Hester et al.*, 1990]. Poorly understood are geomechanical conditions that make them exploitable reservoirs.

Mudrock units are regionally mapped using seismic methods; however, the ultimate goal is to detect zones where large sustainable, interconnected fracture networks can be artificially induced [*Curtis*, 2002].

[1] Weight percentage of organic carbon in a rock

Wheeler [2009] suggests that rock brittleness, a measure of failure under stress, plays a key role in generating large fracture fairways. In principle, reflection seismic data has the potential to characterize mudrocks because of geomechanical properties such as Young's Modulus and Poisson's Ratio which determine the brittleness and also affect the P- and S- wave velocity (V_P and V_S respectively). However, in practice, recovery of geomechanical properties of a rock matrix from seismic data is non-trivial; a multitude of factors including porosity, pore-fluids, and overburden pressure also have a significant (and sometimes opposing) effect on V_P and V_S. In general, there is a lack of consensus in the literature regarding seismic modeling methods that can be used effectively to predict the elastic velocities in mudrocks. *Lucier et al.* [2010] use a combination of Gassmann fluid substitution and empirical data on hydrocarbon source rock performed by *Vernik and Nur* [1992] to explain the gas saturation in sonic logs from the Haynesville Shale, Louisiana. *Knight et al.* [1998] demonstrate the need of including capillary pressure variations for predicting V_P within shaly sand. *Hall and Alvarez* [2010] proposed a mixing law in approximation to the Biot poro-elastic term which could be used to model any combination of mineral assemblages. *Vanorio et al.* [2010] showed that although anisotropy affects V_P, the effect is more significant at higher pressures; the composition of kerogen-constituting materials with respect to the overburden pressure therefore needs to be accounted while modeling elastic properties of mudrocks.

We present a first principle based effective medium modeling method based on the effective medium model of *Helgerud et al.* [1999] for predicting V_P and V_S of mineral and fluid compositions that resemble natural mudock assemblages; here we provide an overview and guide the reader to the original paper for details. This paper has the

following structure. We first present the theory behind the effective medium modeling method and demonstrate the effect of pressure, porosity, silica content, and free gas saturation on V_P and V_S. Following this we demonstrate estimation of a best-fitting linear trend for the V_P - V_S crossplot from the Woodford Shale in the Mcneff 2-28 well, section 28, T.10N., R.6W., Grady County, Oklahoma. Finally, we assess the reconstructed mudrock assemblage using the Mcneff 2-28 log suite and mineralogical analysis of a cored section of the Upper Woodford from the Campbell 1-34 well, section 34, T.10N., R6W., Grady County, Oklahoma(~1 mile SE of the Mcneff 2-28) and discuss the general applicability of our method. Although our type section is based on the Woodford, which is dominantly siliceous, this method can be potentially extended to any mudrock mineralogy and interstitial fluid type.

.

CHAPTER 3

METHOD

Developing a numerical synthetic model of a rock assemblage involves independent construction of bulk and/or shear moduli of its two main components – the dry rock matrix and the interstitial fluid – followed by their merging using the Gassman relationship [*Gassmann*, 1951]. In this paper, we assume that mineral grains are a) not cemented; b) spherical; and c) randomly packed. For purposes of this paper we also assume that the rock matrix comprises only clay and silica and the pore-fluid comprises only brine and free gas.

The bulk (K_{HM}) and shear (G_{HM}) moduli of dry, randomly packed assemblage of spheres are expressed as:

$$K_{HM} = \left[\frac{n^2 (1-\phi_c)^2 G^2}{18\pi^2 (1-\nu)^2} P \right]^{\frac{1}{3}}, G_{HM} = \frac{5-4\nu}{5(2-\nu)} \left[\frac{3n^2 (1-\phi_c)^2 G^2}{2\pi^2 (1-\nu)^2} P \right]^{\frac{1}{3}} \quad (1)$$

In equation 1, n is the average number of contacts per grain, $\emptyset_c$ is the critical porosity[2], P is the effective pressure (difference between the pore pressure and the overburden pressure), and ν and G are the Poisson's ratio and shear modulus of the solid phase

[2] Mineral grains become suspended at porosity higher than this.

In this study, to simulate the expected compact nature of mudrocks, we use a high coordination number of 12. The model described by Equation (1) is applicable to a single grain mineral packed at the critical porosity thus providing the elastic moduli at this high-porosity endpoint. The other endpoint is at zero porosity where the elastic moduli and density of the sediment are those of the mineral phase itself. In the presence of two or more minerals (e.g., silica and clay, such as in this paper), the moduli can be calculated using the *Hill* [1952] average and mass balance:

$$
\begin{aligned}
K_s &= 0.5 \cdot [\sum_{i=1}^{m} f_i K_i + (\sum_{i=1}^{m} f_i / K_i)^{-1}], \\
G_s &= 0.5 \cdot [\sum_{i=1}^{m} f_i G_i + (\sum_{i=1}^{m} f_i / G_i)^{-1}], \\
\rho_s &= \sum_{i=1}^{m} f_i \rho_i,
\end{aligned}
\tag{2}
$$

where K_s, G_s, and ρ_s are the bulk and shear moduli and density of the mineral (solid) phase respectively; m is the number of the mineral components; f_i is the volumetric fraction of the i-th component in the solid phase; and K_i, G_i, and ρ_i are the bulk moduli, shear moduli and density of the i-th component respectively. A variety of methods exist in the literature for computing intermediate values of moduli between the critical and the zero porosity endpoint depending on the grain geometry and interaction at grain contacts [*Wang*, 2001]. In this paper, we assume that in response to the overburden stress the pore shapes do not change and the fluids can travel freely within the pores maintaining a constant pore-pressure; this state is best described by the modified upper Hashin-Sthrikman bound [*Hashin and Shtrikman*; 1963; *Mavko et al.*, 2009]. Consequently, in this paper, the effective pressure, which is also a measure of stress, linearly increases

with depth.

The dry bulk (K_{Dry}) and shear (G_{Dry}) moduli are be expressed as:

$$
\begin{aligned}
K_{Dry} &= \left[\frac{\phi/\phi_c}{K_{HM}+\frac{4}{3}G_s} + \frac{1-\phi/\phi_c}{K_s+\frac{4}{3}G_s}\right]^{-1} - \frac{4}{3}G_s, \\
G_{Dry} &= \left[\frac{\phi/\phi_c}{G_{HM}+Z} + \frac{1-\phi/\phi_c}{G_s+Z}\right]^{-1} - Z, \\
Z &= \frac{G_s}{6}\left(\frac{9K_s+8G_s}{K_s+2G_s}\right).
\end{aligned}
\tag{3}
$$

where K_s and G_s are the bulk and shear moduli of the solid phase and $\varnothing$ is the total porosity. The density of pore-fluid can be then estimated using *Batzle and Wang* [1992] relationship which predicts acoustic velocities and densities of pore fluids for a given ambient pressure and temperature. The moduli for saturated rock are expressed as:

$$
K_{Sat} = K_s\frac{\phi K_{Dry} - (1+\phi)K_f K_{Dry}/K_s + K_f}{(1-\phi)K_f + \phi K_s - K_f K_{Dry}/K_s}, G_{Sat} = G_{Dry}, \tag{4}
$$

where K_f is the bulk moduli of the pore-fluid. The bulk density (ρ_b) is obtained from mass balance as:

$$
\rho_b = (1-\phi)\rho_s + \phi\rho_f, \tag{5}
$$

Finally, the V_p and V_s relate to the elastic moduli (K_{sat} and G_{sat}) and density (ρ_b) as:

$$
K_{sat} + \tfrac{4}{3}G_{sat} = \rho V_p^{\,2}, G_{sat} = \rho V_s^{\,2} \tag{6}
$$

CHAPTER 4

APPLICATION

Using the proposed rock physics methodology, we model V_P and V_S data from the Woodford Shale in the Mcneff 2-28 (Figure 1) with the intention of quantifying the range of three main parameters that are relevant to the exploration potential of a mudrock : mineralogy (Silica versus Clay), porosity range, and gas saturation. As a first step we perform synthetic modeling to appreciate the effects of silica, porosity, and gas saturation individually on V_P and V_S. A "base section" is developed with 5% porosity and 100% clay that has the same thickness (170 ft) and depth (~10,000 ft) as the Woodford in the Mcneff 2-28. For the clay phase computation, we use physical properties of Illite, which is a characteristic Woodford mineral [*Jarvie*, 2008; *Whittington II*, 2009; *Caldwell*, 2011]. In the base section the effective pressure increases linearly with depth and the porosity is held constant at 5%, the pores are brine saturated, and no silica is present in the matrix. V_P and V_S are computed at every 0.5ft depth to resemble depth sampling in the real log.

4.1: EFFECT OF MAJOR PARAMETERS

The V_P and V_S of the base section increases linearly with effective pressure (Figure 2a).

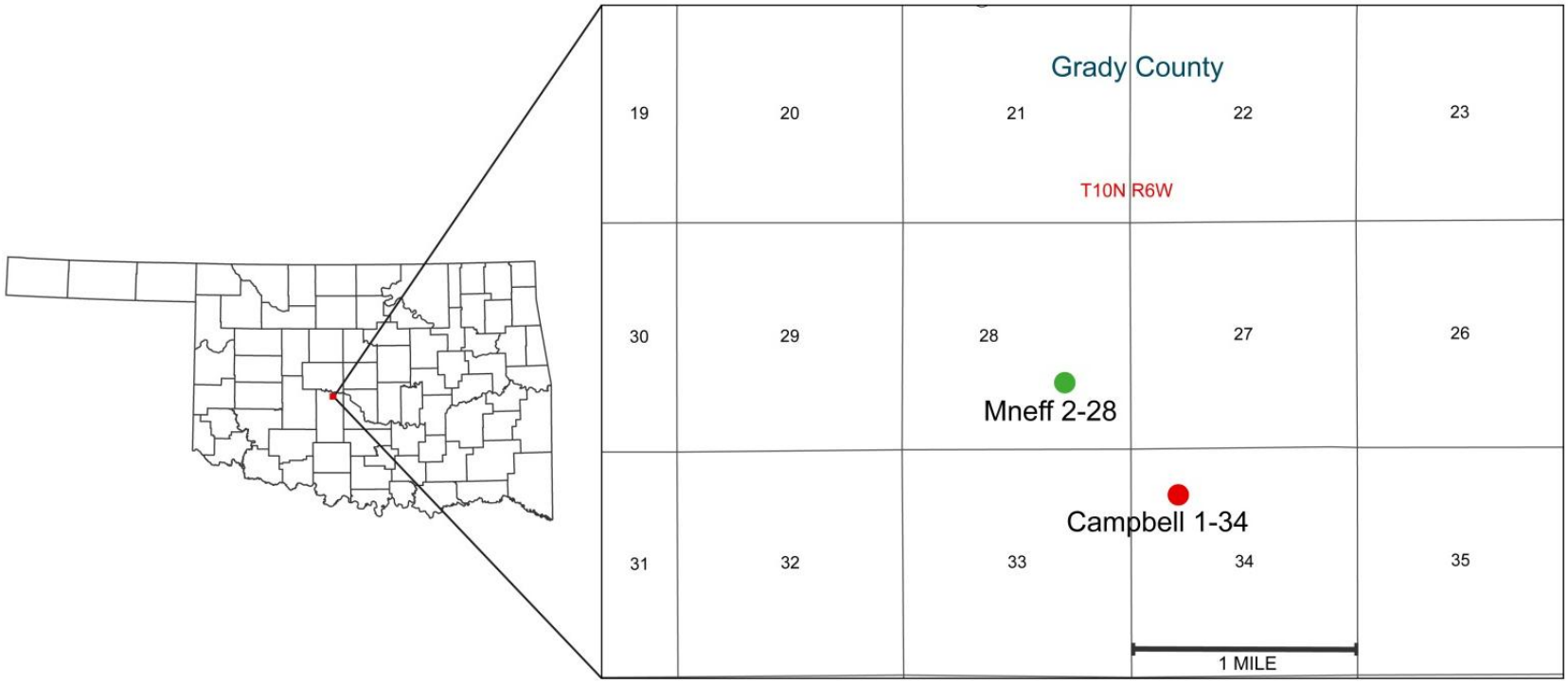

Figure 1: Base map showing location of study area in northern Grady County. Rock physics modeling (Figures 2-4) is demonstrated with V_P-V_S data from the Mcneff 2-28 (green) Modeling results are compared with a cored Upper Woodford interval from the Campbell 1-34 (red)

Next, in the base section, maintaining an increasing effective pressure with depth we increase the bulk porosity (Pink shade; Figure 2b) in steps of 5% up to 30%, bulk silica (Blue shade; Figure 2b) in steps of 0% up to 100%, and bulk gas saturation (Green shade; Figure 2b) in steps of 0% up to 80%. While varying any one of the three parameters the other two parameters are maintained at their base values. Figure 2(b) suggests that V_P and V_S decrease linearly with increasing porosity and increase linearly with increasing silica. The effect of free gas is non-linear; increasing free gas decreases V_P but slightly increases V_S (Figure 2b). This is also reflected in Equations 4 and 5 which suggest that free gas does not change the shear modulus of the saturated rock but decreases the bulk density.

Synthetic modeling results generally agree with literature. The high sensitivity of V_P and V_S to low saturations of free gas (e.g., maximum change in V_P occurs when gas saturation changes from 0% to 20%; Figure 2b) has also been observed by *Lee and Collett* [2006] in gas hydrates settings and by *Lucier et al.* [2011] in shale gas plays. The higher sensitivity of V_P and V_S to changes in porosity as compared to changes in silica (change in porosity from 5% – 30% gives a similar spread in V_P – V_S as change in silica from 0 – 95%; Figure 2b) has also been previously indicated by *Eastwood and Castagna* [1987] with log data and *Tosaya and Nur* [1982] with numerical models. An important aspect of synthetic models in Figure 2 is the opposing effect of porosity and silica (Figure 2b) on V_P and V_S which makes it likely that siliceous, porous sections (i.e., mechanically favorable zones) within a mudrock unit may not be differentiable from non-siliceous, non-porous sections (i.e., mechanically unfavorable zones) using elastic velocities. Opposing effect of silica and porosity on elastic velocities has previously been documented by *Castagna et al.* [1985] with worldwide mudrocks samples.

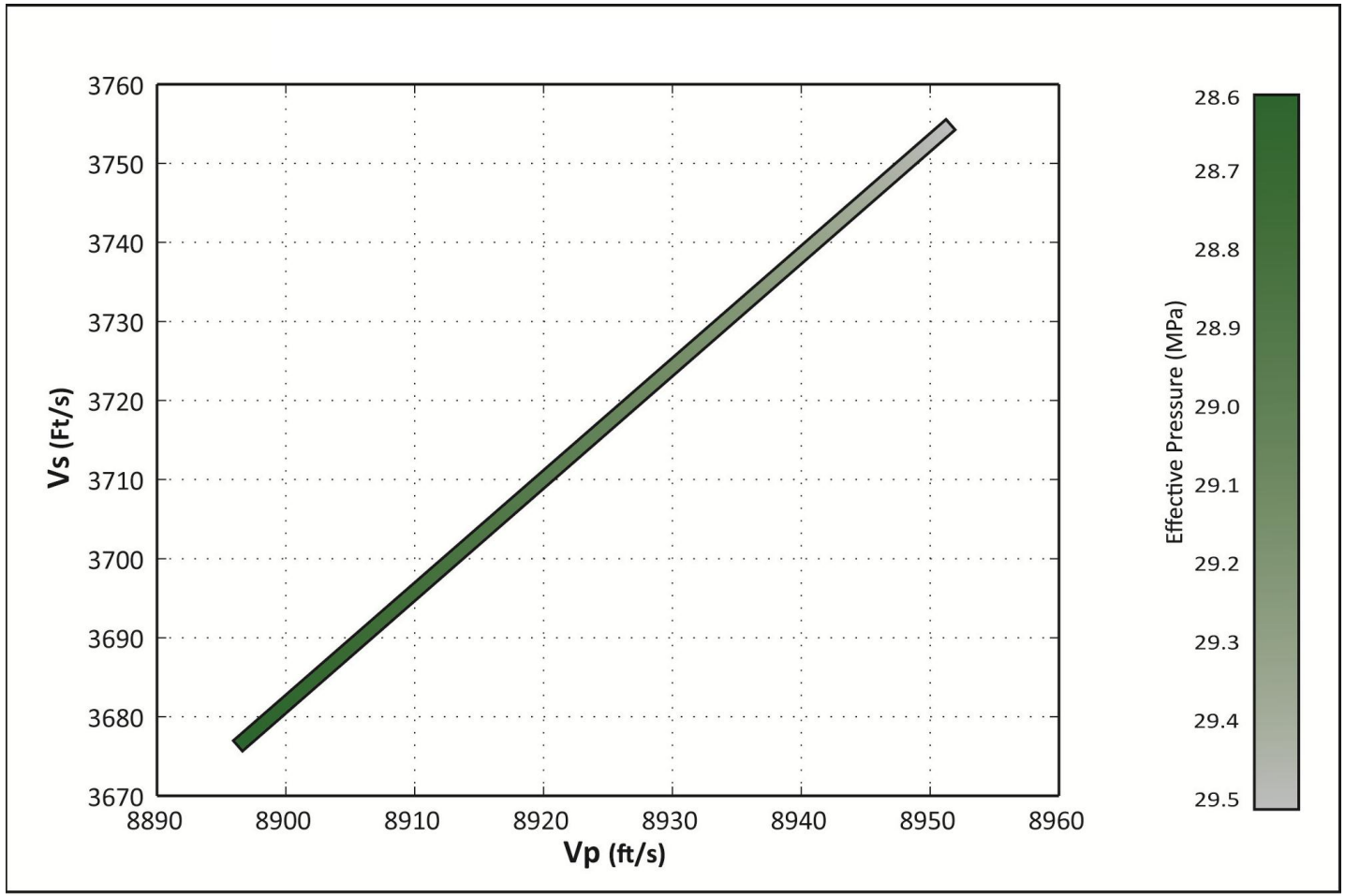

Figure 2: (a) Result of changing effective pressure with depth in the "base section". Pressure will be lowest at the top of the Woodford and increase with depth. This model has no silica in the matrix and tends agree with the theory that effective pressure will increase with depth.

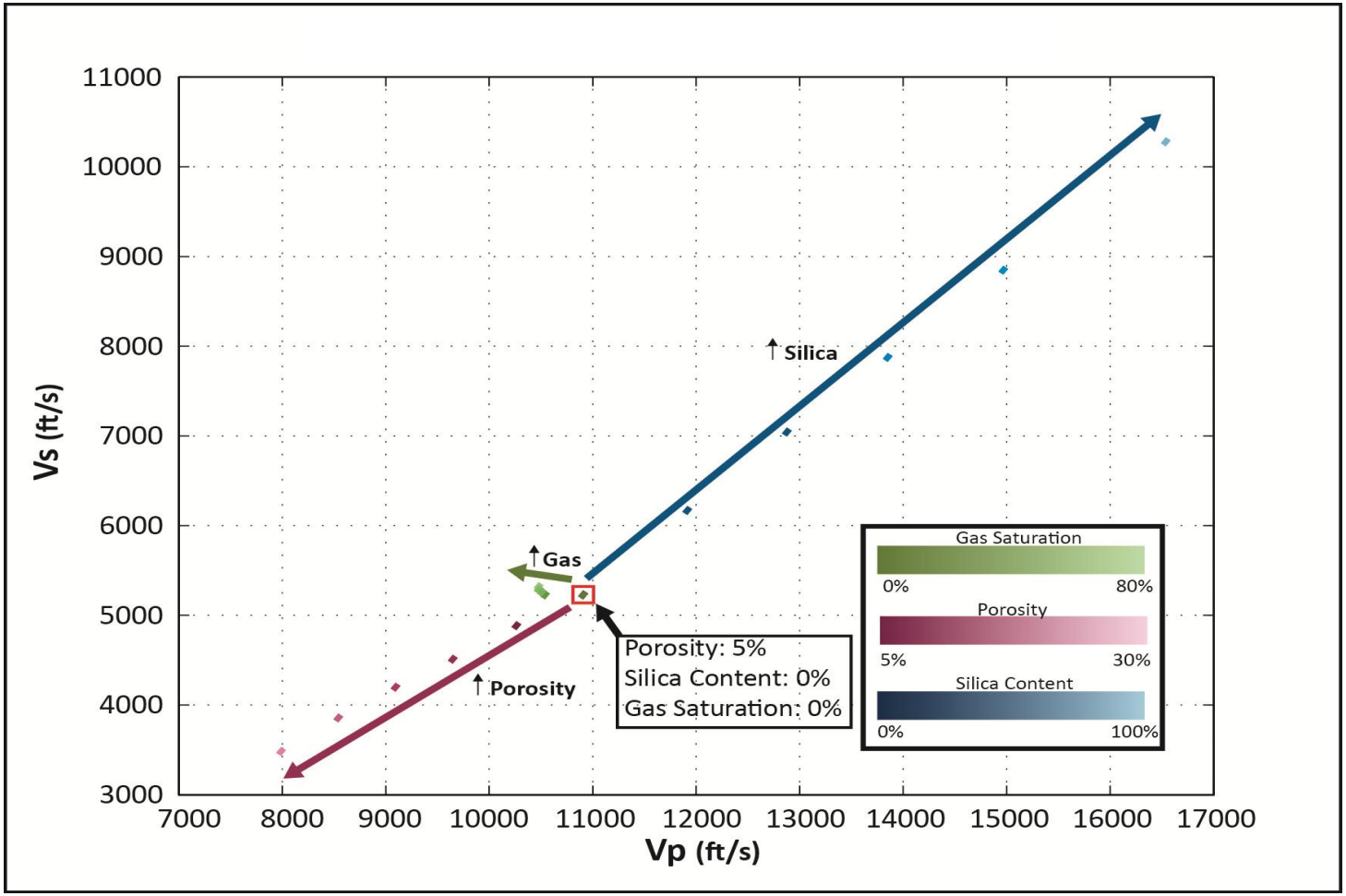

Figure 2: (b) Modeled Vp-Vs bulk trends. Shows general trends as they are changed from a base model (red box), independently while other parameters remain constant. Silica is increased in steps of 5% from 0%-100%, porosity is increased in steps of 5% from 5%-30%, and gas saturation is increased in steps of 5% from 0-80%. Arrows show basic trends that the increase or decrease of each parameter will have

4.2: REAL DATA MODELING

Using the synthetic results from Figure 2, we predict a linear $V_P - V_S$ trend which best fits the $V_P - V_S$ data crossplot from the Mcneff 2-28 ; our intent is not to be able to predict the individual data points but rather estimate generic changes in silica, porosity, and gas saturation from the top to the base of the Woodford which will yield the best-fitting trend. Further, for simplicity and ease of interpretation, we predict the $V_P - V_S$ trends only with linear variations of silica, porosity, and gas saturation in depth.

A visual comparison of synthetic results (Figure 2) and real data (Figure 3) provides first-order estimates of silica. In the real data, highest V_P occurs at the shallowest depths and vice-versa (Figure 3); this requires a higher silica at the Woodford top compared to its base in order to counter the influence of effective pressure (Figure 2a). No speculation on the gas content can be made at this state. We make an initial estimate of porosity in the 10 – 20% range from contemporary studies on the Woodford [*Blackford*, 2007; *Caldwell*, 2011; *Comer*, 2005; *Jarvie*, 2008]. Next, in a heuristic manner, we perturb the base model with multiple linearly decreasing silica trends, linearly increasing and decreasing porosity trends, and linearly decreasing gas saturation trends. For each trend we compute the Root Mean Square Error (E_{RMS}) between the predicted and the observed V_P and V_S values as:

$$E = \frac{1}{n}\sqrt{\sum_{i=1}^{n}\left(V_P^{Pi} - V_P^{Oi}\right)^2 + \sum_{i=1}^{n}\left(V_s^{Pi} - V_s^{Oi}\right)^2} \tag{7}$$

where n is the number of data points, and the superscripts Pi and Oi denote the i^{th} predicted and observed data point.

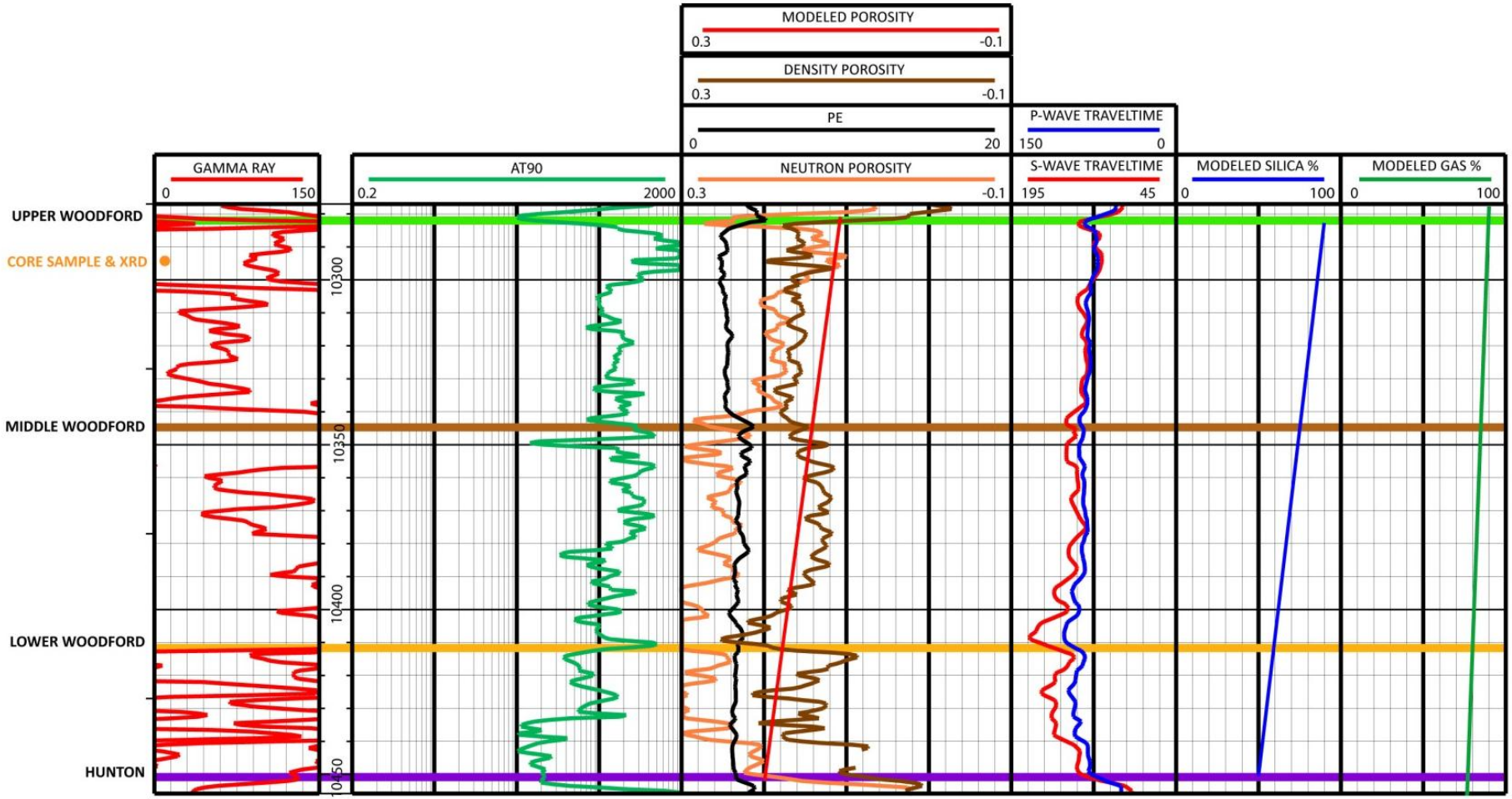

Figure 3: Mcneff 2-28 log suite: Gamma ray (track 1; red), deep resistivity (track 2; green), Density porosity (track 3; brown), Neutron porosity (track 3; orange), Photoelectric (track 3; black), P- wave arrival times (track 4; blue), and S-wave arrive times (track 4; red). Estimated porosity (track 3; red), silica (track 5; blue) and gas saturation (track 6; green) correspond to the best fitting trend (T5; Table1). The Upper, the Middle, and the Lower Woodford intervals are interpreted based on gamma ray and resistivity.

CHAPTER 5

RESULTS

Five representative permutations of silica, porosity and gas saturation depth profiles are presented in Table 1 with their associated RMS errors. These trends are shown on a $V_P - V_S$ crossplot and overlain on the log data for a visual comparison. The minimum error, best-fit mudrock model (T5; Table 1) comprises silica decreasing linearly from 90% at the top to 50% at the bottom; porosity increasing linearly from 10% at the top to 21% at the bottom; and gas saturation decreasing linearly from 90% at the top to 85% at the bottom of the base section. In general, the best-fitting trend implies that the Woodford Shale in the Mcneff 2-28 has relatively high overall silica content (> 60%), intermediate porosity (10 -21%), and high gas saturation (85 - 90%). Porosity variation for the best-fit $V_P - V_S$ trend (Figure 4a) appears to be a reasonable linear approximation to the model that uses density-porosity log values from the Mcneff 2-28 instead of using the linear porosity trend (Figure 4b) indicating that our modeling is reasonable. A considerable reduction in RMS error can be achieved by using the real porosity log (T6; Table 1).

Trend	Silica Content		Porosity		Gas Saturation		Error
	Top	Base	Top	Base	Top	Base	
1	85%	50%	12%	22%	90%	85%	1647.5
2	95%	50%	10%	21%	90%	85%	1134.8
3	85%	55%	10%	21%	90%	85%	1053.2
4	90%	50%	10%	21%	90%	40%	948.7
5	90%	50%	10%	21%	90%	85%	908.9
6	90%	50%	Density-Porosity		90%	85%	435.5

Table 1: Silica, porosity, and gas saturation trends and associated RMS error.

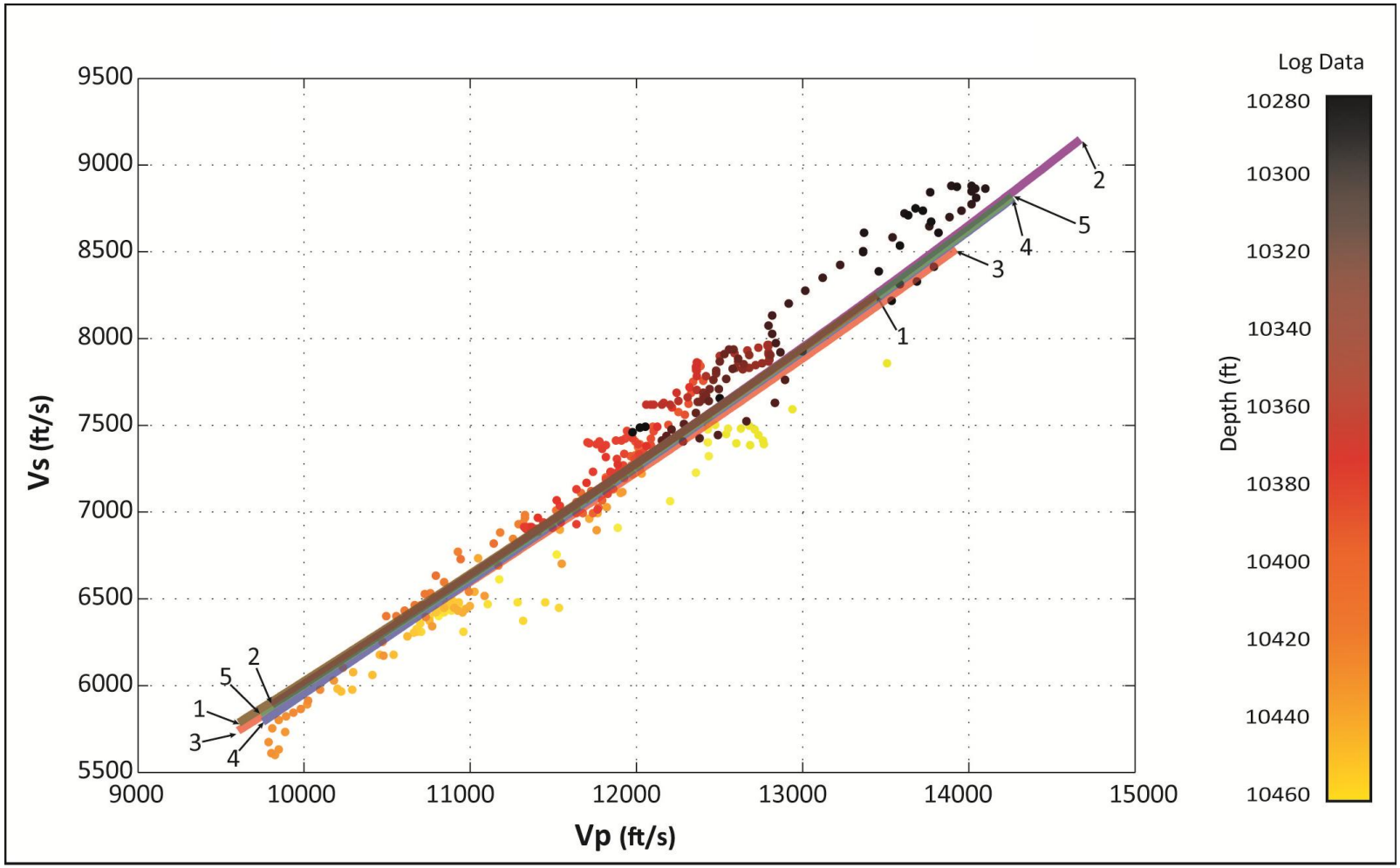

Figure 4: (a) Vp-Vs log data overlain with modeled trends from table 5. Trends are transparent and labeled with arrows on the top and base of each trend for comparison. Trend 5 (green) is the trend of the best fit associated with the lowest RMS error. The log data also displays a depth colorbar and shows that the Woodford has a relatively clear decrease in both Vp and Vs velocities with depth.

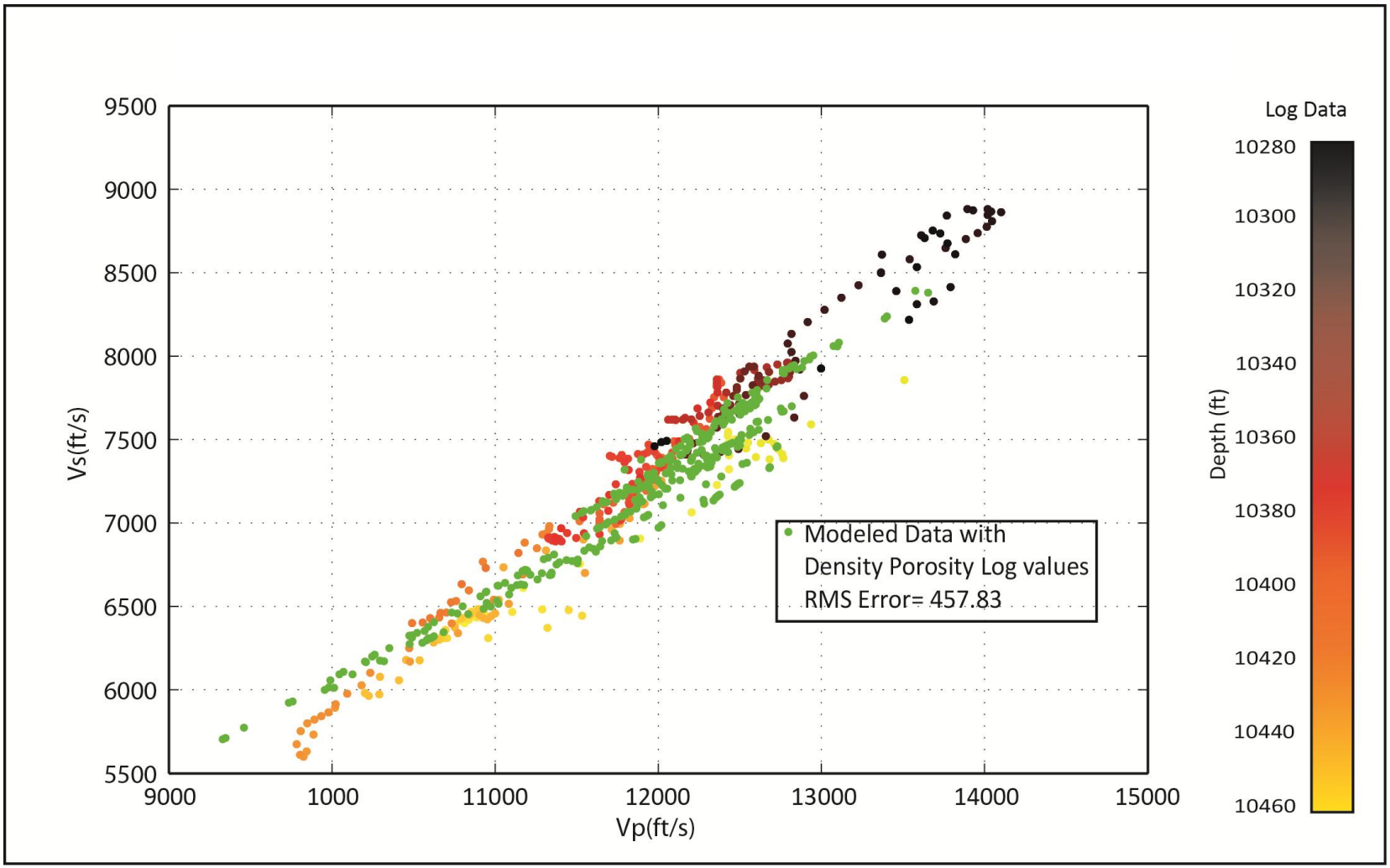

Figure 4: (b) Vp-Vs log data overlain with a modeled trend that uses porosity values from the density porosity log (green) instead of a linear porosity trend.

CHAPTER 6

DISCUSSION

From a sequence stratigraphic perspective, the Woodford is divided into thee sub-units – the Upper, the Middle, and the Lower [*Slatt and Abousleiman*, 2011]. In the Mcneff 2-28 three sub-units can be identified based on the gamma ray log and resistivity character [*Blackford,* 2007]. High silica content in the Upper Woodford in the Mcneff 2-28 is also supported by neutron-porosity and photoelectric (PE) logs (Figure 3). In the presence of clay, the neutron-porosity log has higher values than the corresponding density-porosity log [*Asquith and Krygowski*, 2004]. Thus, a visual inspection of the Mcneff 2-28 neutron-porosity suggests that the proportion of clay in the Woodford matrix appears to be increasing with depth. Since the Woodford in the Anadarko Basin mainly comprises clay and silica [*Caldwell,* 2011], the neutron-porosity log can also be indicative of decreasing silica with depth which supports our modeling. Additional support for high silica in the upper Woodford comes from the Mcneff 2-28 Photoelectric (PE) log. PE values of Illite are ~3.2 and quartz are ~1.82 [*Doveton*, 2003]. The PE log in the upper Woodford is below 2 indicating high silica and in the Middle and Lower Woodford is 2 – 3 indicating an increase in clay content as compared to the Upper Woodford.

High silica in the Upper Woodford can also be supported by a core sample from the Campbell 1-34 (Figure 1) located ~1 miles SE of the Mcneff 2-28 which shows high conchoidal fracturing (Figure 5a), a characteristic of microcrystalline quartz dominated Woodford [*Portas and Slatt*, 2010]. A more detailed analysis of the matrix mineralogy through X-ray diffraction (XRD) show significant peaks in quartz mineralogy (Figure 5b) further supporting high (>50%) silica. In addition to XRD, as stated earlier, mineralogy is the main controller of mechanical properties such as Young's Modulus and Poisson's Ratio. Using V_P-V_S log data, these mechanical properties are calculated and plotted against one another. Data points are colored with Woodford Stratigraphy: Upper , Middle , and Lower (Figure 6). Silica is more brittle than clay and will be characterized by a low Poisson's Ratio and high Young's Modulus. Interpretation of Figure 6 shows that there is a clear linearly increasing brittle trend which is associated with increasing silica content and a linearly increasing ductile trend which is associated with increasing clay content. This trend provides further reinforcement of the modeled data and the overall linear decrease in silica content from Upper to Lower Woodford. [*Harris et al.*, 2010] have also analyzed mechanical properties of the Woodford Shale from the Permian Basin and suggest a similar increase in quartz content, from 41% in the Lower Woodford to 81% in the Upper Woodford. In regard to the calculated RMS error, it is difficult to compare the errors in this study to conventional error analysis. This is because a linear trend is being compared to a scatter of data points the overall error will be high. Although the best fit modeled trend has exceptionally high RMS error values, it is still the lowest error trend that is obtained using this particular method. Some uncertainty in this study remains with regards to the predicted free gas saturation mainly for two reasons. First,

from a modeling perspective the sensitivity of elastic velocity to variations in free gas decreases with increasing saturation. As a result the RMS error changes slightly even with significant change in gas saturation, e.g., Trends 4 and 5 in Table 1 show that reduction in gas saturation in lower Woodford by ~50% increases the RMS error by ~5% only. Second, from a mineralogical perspective, significant amounts of gas can exist as an adsorbed phase in the TOC [*Holmes et al.,* 2011]; the adsorbed gas effects elastic velocities much like free gas in pore spaces [*Zhu et al.*, 2011] but cannot be quantified directly through conventional well log analysis or production testing. Recoverable free gas saturations in shale plays can range anywhere from 15 to 80% [*Curtis*, 2002] making it likely that the gas saturation in the Upper Woodford suggested by our modeling is realistic. Further, [*Lewis et al.*, 2004] shows that gas adsorption is more efficient at pressures less that 1500 psi, while at higher pressures, such in the Mcneff-28 with pressures at ~4200 psi, the gas may be dominantly present as a free phase; suggesting the estimated free gas saturations which makes the Woodford in general, and the Upper Woodford in particular, in the Mcneff 2-28 prospective.

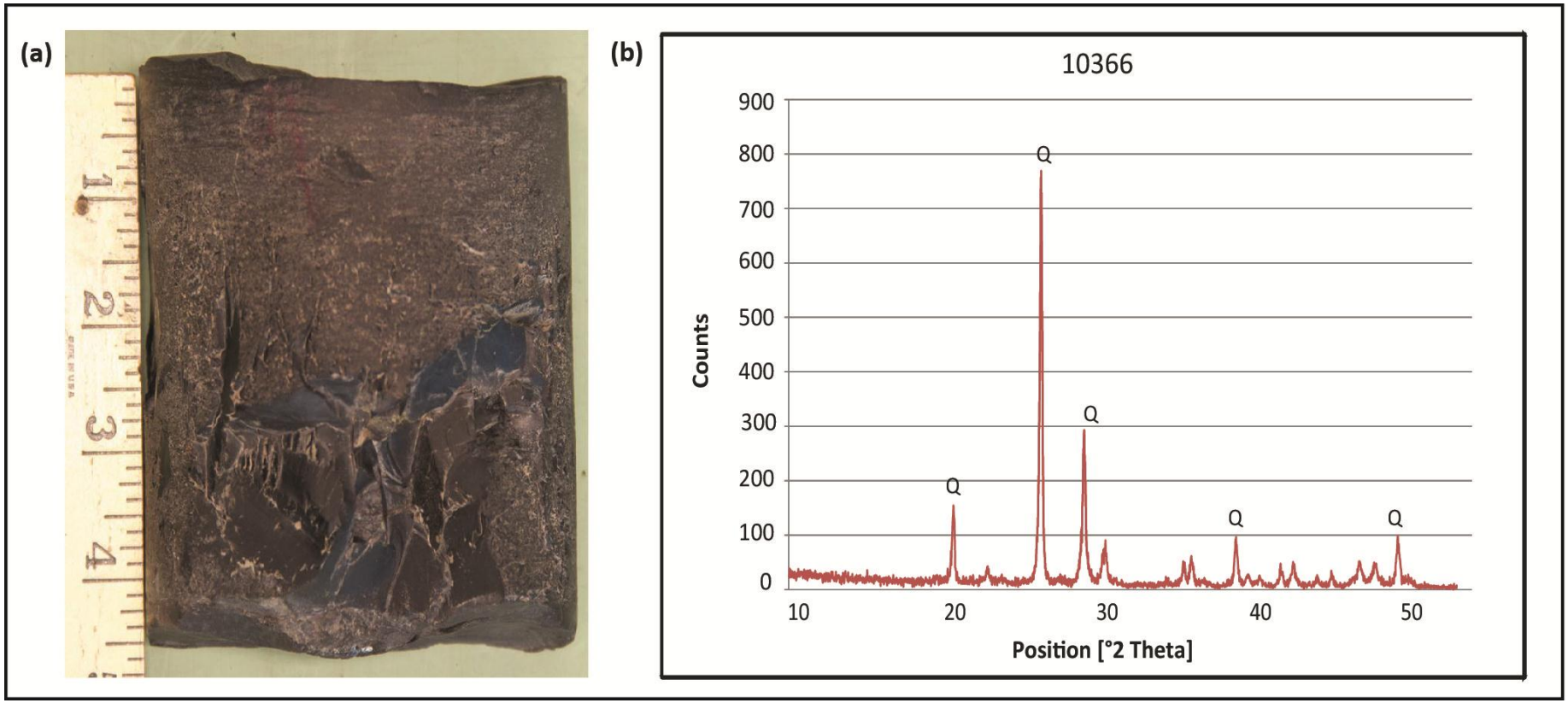

Figure 5: (a) Core photo of sample of Upper Woodford from the Campbell 1-34 **(b)** XRD plot generated from a the sample pictured in (a). All peaks of significant intensity are quartz (Q), clay is minimal and clay mineralogy cannot be quantified.

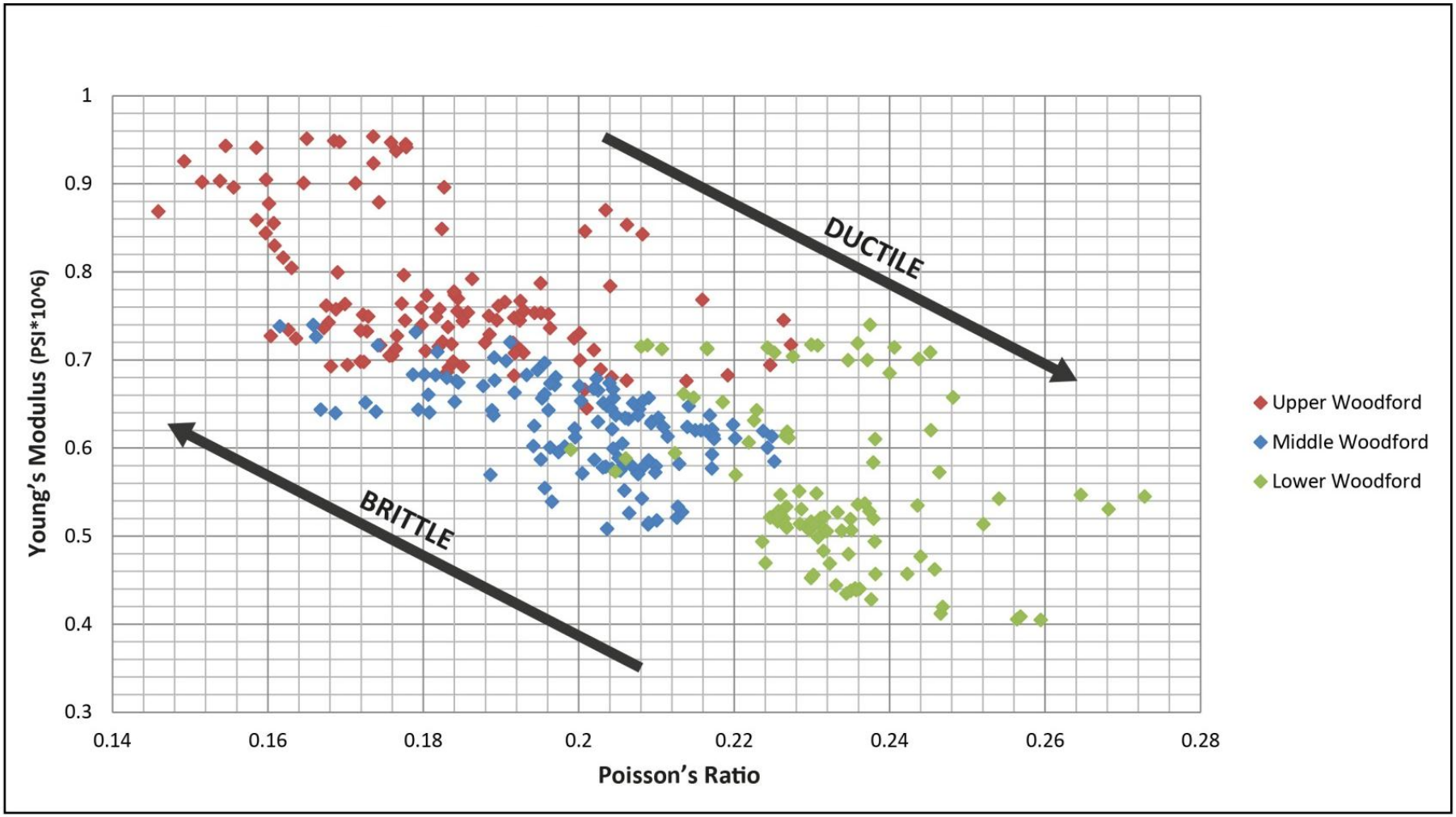

Figure 6: Mechanical stratigraphy of the Woodford interval in the Mcneff 2-28. Young's Modulus and Poisson's Ratio are calculated using actual log data. Woodford stratigraphy identified from gamma ray and resistivity is denoted by Upper (red), Middle (blue), and Lower (green)

CHAPTER 7

CONCLUSION

A first principle based rock physics modeling methods for testing the effect of silica, porosity, and gas saturation on V_P and V_S in mudrocks assuming a two-phase matrix (clay and silica) and a two-phase pore fluid (brine and gas) is presented. Increasing silica increases both V_P and V_S and increasing porosity decreases both V_P and $V_{S;}$ as a result, multiple combinations of silica content and porosity can yield similar V_P and V_S. Increasing free gas decreases V_P while only slightly increasing $V_{S.}$ Generic depth profiles of silica, porosity, and free-gas saturations within 170 ft thick Woodford section in the Mcneff 2-28 are estimated by minimizing the Root Mean Square Error between the predicted and observed V_P and V_S values. The Woodford model with minimum error is associated with decreasing silica and free gas (90 – 50% and 90 – 85% respectively) and increasing porosity (10 – 20%) with depth. Comparison of the modeled porosity trend with the density porosity log is agreeable. Moderately high silica content of the Upper Woodford is confirmed by core analysis and X-Ray Diffraction of a sample from the Campbell 1-34 located ~1 mile southeast of the study well. An overall decrease in silica from the top to the base of the Woodford are indicated by neutron density and photo electric logs which support the least error modeled silica trend.

Mechanical properties of the log data show a linearly increasing brittle trend and a linearly increasing ductile trend which also affirms the modeled silica values. The estimates on gas saturation, although realistic, are least constrained. Results strongly suggest that the Woodford Shale in the Mcneff 2-28 locality is potentially prospective.

REFERENCES

Asquith, G., and D. Krygowski (2004), Basic Well Log Analysis *AAPG Methods in Exploraton Series, Second Edition*.

Batzle, M., and Z. Wang (1992), Seismic properties of pore fluids, *Geohphysics, 57*(11), 1396-1408.

Blackford, M. A. (2007), Electrostratigraphy, Thickness, and Petrophysical Evaluation of the Woodford Shale, Arkoma Basin, Oklahoma, *Thesis*. Oklahoma State Univ.

Blatt, H., R. J. Tracy, and B. Owe (2005), *Petrology: Igneous, Sedimentary and Metamorphic*, 3rd ed., W. H. Freeman.

Caldwell, C. D. (2011), Lithostratigraphy of the Woodford Shale, Anadarko Basin, West-Central Oklahoma, *Oklahoma Geological Survey Shales Moving Forward Workshop, July 21, 2011*.

Castagna, J. P., M. L. Batzle, and R. L. Eastwood (1985), Relationships bewtween compressional-wave and shear-wave velocities in clastic silicate rocks, *Geophysics, 50*(4), 571-581.

Charpentier, R. R., and T. Cook (2010), Applying probabilistic well-performance parameters to assessments of shale-gas resources. USGS. Report 1151

Comer, J. (2005), Facies distribution and hydrocarbon production potential of Woodford Shale in the southern midcontinent, *Oklahoma Geological Survey Circular, 110*, 51-62.

Curtis, J. B. (2002), Fractured shale-gas systems, *AAPG Bulletin, 86*(11), 1921-1938.

DOE (2009), Modern Shale Gas Development in the United States: A Primer, edited by O. o. F. Energy, Department of Energy.

Doveton, J. (2003), Reading the Rocks from Wireline Logs, *Kansas Geological Survey, Oil and Gas Information*.

Eastwood, R. L., and J. P. Castagna (1987), Interpretation of Vp/Vs ratios from sonic logs, *SEG, Geophysical Development Series*, 139-153

Gassmann, F. (1951), ELASTIC WAVES THROUGH A PACKING OF SPHERES, *Geophysics*, *16*(4), 673-685.

Grainger, P. (1984), The classification of mudrocks for engineering purposes, *Quaterly Journal of Engineering Geology & Hydrogeology*, *17*(4), 381-387.

Hall, J., and E. Alvarez (2010), Overcoming the limitations of rock physics modelling in porous rock with complex mineralogy, *Society of Petrophysicists and Well Log Analysts 51st Annual Logging Symposium, June 19-23, 2010*.

Harris, N. B., J. L. Miskimins, and C. A. Mnich (2011), Mechanical anisotrophy in the Woodford Shale, Permian Basin: Origin, magnitude, and scale, *The Leading Edge*, *March 2011*.

Hashin, Z., and S. Shtrikman (1963), A variational approach to the theory of the elastic behaviour of multiphase materials, *Journal of the Mechanics and Physics of Solids*, *11*(2), 127-140.

Helgerud, M.B., J. Dvorkin, A. Nur, A Sakai, and T. Collett (1999), Elastic-wave velocity in marine sediments with gas hydrates: Effective medium modeling, *Geophysical Research Letters*, 26(13), 2021-2024.

Hester, T. C., and J. W. Schmoker (1987), Formation resistivity as an indicator of oil generation in black shales, *AAPG Bulletin*, *71*.

Hester, T. C., J. W. Schmoker, and H. L. Sahl (1990), Log-Derived Regional Source-Rock Characteristics of the Woodford Shale, Anadarko Basin, Oklahoma, *U.S. Geological Survey Bulletin*, *1866-D*(Evolution of sedimentary basins).

Hill, R. (1952), The Elastic Behaviour of a Crystalline Aggregate, *Proceedings of the Physical Society. Section A*, *65*(5).

Holmes, M., D. Holmes, and A. Holmes (2011), A petrophysical model to estimate free gas in organic shales, *AAPG Search and Discovery, July 2011*(Artilcle #40781).

Jarvie, D. (2008), Geochemical Characteristics of the Devonian Woodford Shale, *Oklahoma Geological Survey, Oklahoma Gas Shales Workshop, October 22, 2008*.

Knight, R., J. Dvorkin, and A. Nur (1998), Acoustic signatures of partial saturation, *Geophysics, Vol 63*(No. 1), 132-138.

Lee, M. W., and T. S. Collett (2006), Gas hydrate and free gas saturations estimated from velocity logs on Hydrate Ridge, offshore Oregon, USA, *Trehu, A.M., Bohrmann,G.,Torres,M.E., and Colwell F.S. (Eds.) Proc. ODP, Sci. Results, 204*, 1-25.

Lewis, R., D. Ingraham, M. Pearcy, J. Williamson, W. Sawyer, and J. Frantz (2004), New Evaluation Techniques for Gas Shale Reservoirs, *Schlumberger Reservoir Symposium*.

Lucier, A. M., R. Hofmann, and T. Bryndzia (2011), Evaluation of variable gas saturation of acoustic log data from the Haynesville Shale gas play, NW Louisiana, USA, *The Leading Edge, March 2011*.

Mavko, G., T. Mukerji, and J. Dvorkin (2009), The rock physics handbook: tools for seismic analysis of porous media-2nd ed., *Cambridge University Press 2009*.

Portas, R. M., and R. Slatt (2010), Characterization and Origin of Fracture Patterns in a Woodford Shale Quarry in Southeastern Oklahoma for Appliation to Exploration and Development, *AAPG Search and Discovery, November*.

Slatt, R. M., and Y. Abousleiman (2011), Merging sequence stratigraphy and geomechanics for unconventional gas shales, *The Leading Edge*, *30*(3), 274-282.

Tosaya, C., and A. Nur (1982), Effects of Diagenesis and Clays on Compressional Velocities in Rocks, *Geophysical Research Letter*, *9*(1), 5-8.

Vanorio, T., T. Mukerji, and G. Mavko (2011), Emerging methodologies to characterize the rock physics properties of organic-rich shales, *The Leading Edge, March 2011*.

Vernik, L., and A. Nur (1992), Ultrasonic velocity and anisotropy of hydrocarbon source rocks, *Geophysics*, *57*(5), 727-735.

Wang, Z. (2001), Fundamentals of seismic rock physics, *Geophysics*, *66*(2).

Wheeler, D. (2009), It all starts with the rock!, *Ohio OIl and Gas Association Fall Technical Conference, October 20, 2009.*

Whittington II, R. A. (2009), Clay Mineralogy and Illite Crystallinity in the Late Devonian to Early Mississippian Woodford Shale in the Arbuckle Mountains, Oklahoma, USA, Paper 13, Geosciences thesis, Georgia State University, Atlanta.

Zhu, Y., E. Liu, A. Martinez, M. A. Payne, and C. E. Harris (2011), Understanding geophysical responses of shale-gas plays, *The Leading Edge, March 2011*.

VITA

Brian Henry Varacchi

Candidate for the Degree of

Master of Science

Thesis: ROCK PHYSICS AND MECHANICAL STRATIGRAPHY OF THE WOODFORD SHALE, ANADARKO BASIN, OKLAHOMA

Major Field: Geology

Biographical:

Personal Data: Born at Tinker AFB, Midwest City, Oklahoma, on August 2, 1986, to parents Henry and Tracey Varacchi.

Education: Received Bachelor of Science degree in geology at Oklahoma State University, Stillwater, Oklahoma in 2009. Completed the requirements for the Master of Science in Geology at Oklahoma State University, Stillwater, Oklahoma in December, 2011.

Experience: Summer Inter at Halliburton Energy Services (2007); Field Engineering Intern at Halliburton Energy Services (2008); Geology/Geophysics Intern at Laredo Petroleum, Inc. (2010); Teaching assistant at Oklahoma State University (2008-2011)

Professional Memberships: American Association of Petroleum Geologists (AAPG); Society of Exploration Geophysicists (SEG); Oklahoma City Geological Society (OCGS); Tulsa Geological Society (TGS); Oklahoma State University Geological Society (OSUGS)

Name: Brian Henry Varacchi Date of Degree: December, 2011

Institution: Oklahoma State University Location: Stillwater, Oklahoma

Title of Study: ROCK PHYSICS AND MECHANICAL STRATIGRAPHY OF THE WOODFORD SHALE, ANADARKO BASIN, OKLAHOMA

Pages in Study: 29 Candidate for the Degree of Master of Science

Major Field: Geology

Scope and Method of Study: This study was performed to evaluate the mechanical stratigraphy of the Woodford Shale to determine the brittle and ductile components. In order to determine the factors that control the brittle components, we use first principle base effective medium modeling for predicting V_P and V_S of mineral and fluid assemblages that resemble natural mudrocks. The effective medium modeling is used first to demonstrate effect of pressure, porosity,silica content, and gas saturation independently. Using real V_P and V_S data, a stepwise construction of a background model is constructed and compared to the observed data.

Findings and Conclusions: A mechanical stratigraphic framework is developed and corresponds with the petrophysical stratigraphy identified on well logs. Initial models suggest that V_P and V_s (a) decreases linearly with increasing porosity, and (b) increases linearly with increasing silica content. Effect of gas saturation has a decrease on V_P and a slight increase in V_S. This rock physics modeling method is used to estimate the best fitting V_P-V_S trend to observed log data. Modeling suggests that Woodford at this location has high but decreasing silica content with depth (90-50%), low but increasing porosity with depth (10-21%), and high but decreasing gas saturation with depth (90-85%). Comparison of modeled porosity and silica content with density porosity logs, neutron porosity logs, PE logs; XRD data; and mechanical stratigraphy suggests that the rock physics model developed is reasonable.

ADVISER'S APPROVAL: Dr. Priyank Jaiswal